Three-Dimensional Visualization of FKBP12.6 Binding to an Open Conformation of Cardiac Ryanodine Receptor

Manjuli Rani Sharma,* Loice H. Jeyakumar,‡§ Sidney Fleischer,† and Terence Wagenknecht*†
*Wadsworth Center, New York State Department of Health and †Department of Biomedical Sciences, School of Public Health, State University of New York at Albany, Albany, New York 12201-0509; ‡Department of Biological Sciences, Vanderbilt University, Nashville, Tennessee 37235; and §Department of Medicine, Division of Gastroentrology, Vanderbilt University Medical Center, Nashville, Tennessee 37232

ABSTRACT The cardiac isoform of the ryanodine receptor (RyR2) from dog binds predominantly a 12.6-kDa isoform of the FK506-binding protein (FKBP12.6), whereas RyR2 from other species binds both FKBP12.6 and the closely related isoform FKBP12. The role played by FKBP12.6 in modulating calcium release by RyR2 is unclear at present. We have used cryoelectron microscopy and three-dimensional (3D) reconstruction techniques to determine the binding position of FKBP12.6 on the surface of canine RyR2. Buffer conditions that should favor the "open" state of RyR2 were used. Quantitative comparison of 3D reconstructions of RyR2 in the presence and absence of FKBP12.6 reveals that FKBP12.6 binds along the sides of the square-shaped cytoplasmic region of the receptor, adjacent to domain 9, which forms part of the four clamp (corner-forming) structures. The location of the FKBP12.6 binding site on "open" RyR2 appears similar, but slightly displaced (by 1–2 nm) from that found previously for FKBP12 binding to the skeletal muscle ryanodine receptor that was in the buffer that favors the "closed" state. The conformation of RyR2 containing bound FKBP12.6 differs considerably from that depleted of FKBP12.6, particularly in the transmembrane region and in the clamp structures. The x-ray structure of FKBP12.6 was docked into the region of the 3D reconstruction that is attributable to bound FKBP12.6, to show the relative orientations of amino acid residues (Gln-31, Asn-32, Phe-59) that have been implicated as being critical in interactions with RyR2. A thorough understanding of the structural basis of RyR2-FKBP12.6 interaction should aid in understanding the roles that have been proposed for FKBP12.6 in heart failure and in certain forms of sudden cardiac death.

INTRODUCTION

Ryanodine receptors (RyRs) are intracellular calcium channels that are found in many mammalian cell types, but they are particularly enriched in the sarcoplasmic reticulum (SR) of striated muscle where they play a key role in excitation-contraction coupling (reviewed in Bers (1) and Fill and Copello (2)). RyRs are the largest ion channels known, existing as homotetramers whose constituent subunit contains ~5000 amino acid residues. Of the three known isoforms of RyR, isoform 2 (RyR2) is the main isoform in heart muscle (3). RyRs often copurify with a tightly bound copy of a modulator protein, either a 12- or a 12.6-kDa isoform of FK506-binding protein, an immunophilin that exhibits *cis-trans* peptidyl-prolyl isomerase activity (2) and that can be considered as a second integral subunit of RyR. In mammalian heart, RyR2-FKBP12.6 predominates over RyR2-FKBP12, and this is particularly true of canine RyR2, which has very low affinity for FKBP12 (4–6). The stoichiometry of binding has been known to be four moles of FKBP per mole of tetrameric RyR (i.e., one mole FKBP per mole RyR subunit) (4–6). RyR1s (skeletal muscle isoform) from various classes of vertebrate were found to be associated with FKBP 12, although in vitro experiments show that they are capable of binding/exchanging with both isoforms of FKBP (7,8). The precise role played by FKBP12/FKBP12.6 in the functioning of RyRs is currently unclear and controversial, but it is of intense interest, primarily because the proteins have been implicated in the molecular mechanism of heart failure, and possibly other arrhythmias, arising from mutations in RyR2 (9–12).

Experiments conducted in vitro have shown that FKBP12 stabilizes the closed state of the skeletal muscle RyR, thereby preventing inappropriate spontaneous channel openings including, according to some studies, subconductance states that occur in the absence of FKBP12 (13–18). Similar effects of FKBP12.6 on RyR2 functioning have been reported in some (19,20), but not all, laboratories (6,21).

FKBP12/FKBP12.6 has also been implicated in coordinating the activities of RyRs that form contacts with one another in the ordered arrays found at junctional interfaces of the SR with the sarcolemma/transverse tubule network (22,23). In vitro, FKBP12 affects RyR1's interactions with the dihydropyridine receptor, implying a possible role for FKBP12 in E-C coupling (24,25). Another proposed function for FKBP12/FKBP12.6 is to serve as an adaptor to bind the phosphatase calcineurin to RyR1 and RyR2 (26,27), thereby enabling calcineurin to regulate the phosphorylation status of the receptor.

The role of the interaction of FKBP12/FKBP12.6 with RyR in situ is even less clear. Depletion of FKBP12 from skinned skeletal muscle fibers interferes with E-C coupling (28), and expression of recombinant mutated RyR1 that lacks the capacity to bind FKBP12 in a skeletal muscle-derived

Submitted March 25, 2005, and accepted for publication September 20, 2005.

Address reprint requests to Manjuli Rani Sharma, Wadsworth Center, New York State Dept. of Health, Albany, NY 12201-0509. Tel.: 518-474-7895; Fax: 518-474-7992; E-mail: manjuli@wadsworth.org.

0006-3495/06/01/164/09 $2.00

doi: 10.1529/biophysj.105.063503

cell line also affects E-C coupling (29). However, although genetic knockout of FKBP12 is lethal in mice, skeletal muscle is nevertheless functional, although the mice exhibit severe cardiomyopathy. Conflicting results have been reported for mice in which FKBP12.6 has been knocked out, with one laboratory reporting cardiac hypertrophy in male but not female mice (30), and another lab describing a more severe phenotype in which susceptibility to heart failure and sudden cardiac death are enhanced in both male and female mice (12). Nevertheless, although the results of these studies on FKBP12/FKBP12.6 knockout mice differ in detail, all report abnormalities in cardiac function.

Marks and colleagues have proposed a provocative mechanism for the progression of heart failure that involves alterations in the FKBP12.6-RyR2 interaction (31). Specifically, they find that, due to the hyperadrenergic state typical of heart failure, protein kinase A becomes overactive, and the resulting hyperphosphorylation of RyR2 causes FKBP12.6 to dissociate from the receptor. FKBP12.6-depleted RyR2s exhibit an abnormally high probability of the open state during diastole that allows leakage of Ca^{2+} from the SR; this in turn reduces the amount of Ca^{2+} that is available to induce contraction during systole and might also trigger ventricular tachycardia. This model for heart failure is currently being tested, with both evidence for (11) and against (10) it being reported. Intriguingly and seemingly in support of Marks's hypothesis (32,33), Yano and co-workers (34) report that a drug, JTV519, shown previously to prevent FKBP12.6 from dissociating from RyR2, is able to protect canine hearts from cardiomyopathy in experimentally induced heart failure.

Recently, mutations in the human RyR2 have been associated with rare forms of exercise-induced sudden cardiac death, catecholaminergic polymorphic ventricular tachycardia, and arrythmogenic right ventricular dysplasia (35–37). Evidence that these mutated RyR2s are defective in their interactions with FKBP12.6 has been described (9,12,38) but these findings have been challenged (39).

Biochemical characterization of the FKBP12/FKBP12.6 binding site on RyRs has been the subject of numerous investigations. For the RyR1 and RyR3 isoforms, evidence points to a conserved valyl-prolyl motif (amino acid residues 2461 and 2462 in RyR1) as being required for binding of FKBP12/FKBP12.6 (40,41). The FKBP12 binding site has also been mapped on the physical structure of RyR1 to a region at the edge of the cytoplasmic region of the receptor by cryoelectron microscopy (cryo-EM) and three-dimensional (3D) reconstruction of isolated RyR1-FKBP12 complexes (42–44). For RyR2 there is an analogous isoleucyl-prolyl sequence (amino acid residues 2427 and 2428) that has been implicated in binding FKBP12.6 (31), but other studies have additionally implicated contributions from other regions of the RyR2 sequence (45–47). Chen and colleagues find that mutation of Ile-2427 or Pro-2428 does not affect FKBP12.6 binding (46) and, further, that an amino-terminal polypeptide fragment encompassing residues 1–1855 derived from RyR2 is sufficient for binding of FKBP12.6 (47). In light of these apparent differences between the modes of FKBP12 and FKBP12.6 binding to respective RyRs, and also because of the above-mentioned potential importance of the RyR2-FKBP12.6 complex in heart disease, we decided to investigate the FKBP12.6 binding site on RyR2 by 3D cryomicroscopy.

MATERIALS AND METHODS

Immunoaffinity purification of RyR2

An isoform-specific RyR2 rabbit polyclonal antibody was developed using a synthetic peptide whose sequence corresponded to 11 amino acids 4418–4429 of rabbit RyR2 (48). The immunizing protocol and affinity purification of sequence-specific antibodies are similar to that described elsewhere (49).

Affinity-purified RyR2-specific antibody was prebound to an immobilized protein A/G matrix by incubating for 1/2 h at room temperature with gentle mixing. Affinity-purified antibody (200–400 μg) was admixed with protein A/G matrix (~200 μl packed bed volume). RyR2-enriched dog heart SR, prepared according to the method described by Chamberlain and co-workers (50), was used for the purification of RyR2. Cardiac SR (100 mg) was solubilized at 6.0 mg/ml in buffer A (20 mM Na_2PIPES, pH 7.2, 0.6 M NaCl, 0.1 mM EGTA, 0.2 mM $CaCl_2$, 5.0 mM Na_2AMP, 2.0 mM DTT, and 0.6% CHAPS (w/v)/0.3% SBL) for 90 min at 4°C with gentle mixing. The mixture was then centrifuged at 50,000 *g* for 30 min at 4°C to remove insoluble material. The supernatant was diluted fourfold with dilution buffer (Buffer B) containing 20.0 mM Na_2-PIPES, pH 7.2, 0.1 mM EGTA, 0.2 mM $CaCl_2$, 5.0 mM Na_2AMP, 2.0 mM DTT, and 0.3 M sucrose and preabsorbed with 50 μl of the preequilibrated protein A/G matrix for 15 min at 4°C with gentle mixing to remove nonspecifically bound components. After sedimenting at low speed in the cold to remove the matrix, the supernatant was transferred to another container, and RyR2 was selectively immunoadsorbed by incubating, with gentle mixing overnight at 4°C, with the calculated amount of prebound RyR2-specific antibody, i.e., prebound to protein A/G matrix. The prebound RyR2 Ab-protein A/G matrix had been preequilibrated with Buffer B (containing 0.15 M NaCl, 0.15% CHAPS/0.075% SBL) for 30 min at 4°C before addition of RyR2. The amount of antibody matrix used to bind RyR2 was determined by the ryanodine binding activity of the cardiac microsomes. A three- to fourfold excess of antibody, i.e., molar ratio of antibody/total RyR binding equivalents was used. The immune complex containing the RyR2 was then sedimented at low speed and was washed sequentially, first with Buffer B containing 0.15 M NaCl, and 0.5% CHAPS/0.25% SBL, second with Buffer B containing 0.5 M NaCl and 0.5% CHAPS/0.25 SBL, and third with Buffer B containing 0.1 M NaCl and 0.5% CHAPS/0.25% SBL. The elution of the RyR2 was carried out with Buffer B containing 20 mM PIPES (pH 7.2), 0.4 M NaCl, 2 mM DTT, 0.6% CHAPS/0.3% SBL, 0.1 mM EGTA, 0.2 mM $CaCl_2$, 5 mM Na_2AMP and excess of epitope peptide (3.0 mg/ml). The eluate was collected and the pellet was washed again with elution buffer without epitope peptide (posteluate). The elution procedure takes ~1 h in the cold room (4°C). This elution protocol should favor the open state of RyR2 (51). The eluate and posteluate were quick-frozen in liquid nitrogen and stored at −80°C. All the buffers used in the preparations contained the protease inhibitors, leupeptin (1.0 μg/ml), aprotonin (1.0 μg/ml), and phenyl-methylsulfonyl fluoride (40 μM).

SDS-PAGE and Western blot analysis

Dog heart SR, i.e., the source of RyR2 and eluates from the immunoaffinity matrix, and RyR2-FKBP12.6 complexes were analyzed by SDS-PAGE and visualized by Coomassie blue staining. For Western blot analysis after SDS-PAGE, the proteins were transferred to an Immobilon-P membrane for 1 h at 24 mA constant current in blot transfer buffer (48 mM Tris, 39 mM glycine, 1.3 mM SDS, pH 9.2) using Trans-Blot SD Semi-Dry Electrophoretic

Transfer Cell (Bio-Rad, Hercules, CA). The vacant binding sites on the membrane were blocked by incubating the membrane in wash buffer (10 mM Tris-Cl, pH 8.0, 0.55 M NaCl, and 0.05% Tween-20) containing 5% nonfat dry milk protein for 1 h. Then the membrane was incubated with the RyR2 or FKBP12-specific antibody in blocking buffer for 1 h. The membrane was washed three times with wash buffer and then incubated with secondary antibody (goat anti-rabbit IgG) conjugated to alkaline phosphatase in blocking buffer. The membrane was again washed three times with wash buffer and developed with nitroblue tetrazolium (NBT) and 5-bromo-4-chloro-3-indoyl phosphate (BCIP) substrates.

Protein determination

Small quantities of proteins such as purified receptor and purified FKBP12.6 were determined by scanning densitometry. Densitometry was carried out using an automated gel analysis plus image processing system (Technology Resources, Nashville, TN) on the RyR2 band after separation in 7.5% resolving gel (SDS-PAGE) and FKBP12.6 in 12.5% resolving gel and staining with Coomassie blue and making use of an HP Scan Jet 4p Scanner, Hewlett Packard and Visioneer PaperPort Software program. Bovine serum albumin was applied to the SDS-PAGE as the protein standard for calibration.

[^{3}H]Ryanodine binding

Routine high affinity ryanodine binding was determined at 60 nM ryanodine. Ryanodine binding to particulate fractions made use of sedimentation to separate bound from free ryanodine as previously described (49). High affinity ryanodine binding parameters were measured by ryanodine binding isotherms using [^{3}H]ryanodine (~15,000 cpm/pmol, obtained from DuPont, NEN, Boston, MA). The binding assay for solubilized fractions was carried out by polyethylene glycol (PEG) precipitation using equine γ-globulin as carrier protein. The samples, 10 μl aliquots, were incubated for 1 h at room temperature in 50 μl of buffer containing 10 mM HEPES-KOH, pH 7.4, 1.0 M KCl, 25 μM $CaCl_2$, 2 mM DTT, and 5.0 mg/ml γ-globulin, and 60 nM [^{3}H]ryanodine. Then PEG (12.5 μl of 25.0%, w/v) was added to the assay mixture and mixed thoroughly using a vortex mixer, and the free ligand was separated from the bound by sedimenting the pellet in a Beckman (Fullerton, CA) TL-100.1 rotor at 95,000 rpm for 15 min at 4°C. The supernatant was removed by aspiration, and the pellets were rinsed twice with water and then resuspended in 0.2 ml of water. The suspensions were transferred to scintillation vials, in 5.0 ml of Cytoscint (ICN, Cleveland, OH) and the radioactivity was measured in a Beckman LS 5000TD scintillation counter. Nonspecific binding was measured in the presence of 20 μM cold ryanodine.

Source of FBKP12.6

Human recombinant FKBP isoform 12.6 was prepared as described earlier (52) and purified by high-performance liquid chromatography using a TSK G3000SW column (6).

Preparation of RyR2-FKBP12.6 complexes for cryoelectron microscopy

Purified RyR2 (0.15 μM) was incubated at room temperature (23°C) for 45 min with FKBP12.6 (4.7 μM), in either the absence or presence of 50 μM FK506 (19,44). The elution buffer of the RyR2, containing 20 mM PIPES (pH 7.2), 0.4 M NaCl, 2 mM DTT, 0.6% CHAPS/0.3% SBL, 0.1 mM EGTA, 0.2 mM $CaCl_2$, 5 mM Na_2AMP, that favors an open state of receptor, was used in preparation of the above RyR2-FKBP12.6 complexes. Cryo-EM grids containing frozen-hydrated protein were prepared as described previously (53). We refer to the complex of RyR2 that was incubated with excess FKBP12.6 as ''RyR2 (+FKBP)'' and the drug-treated sample, which dissociates FKBP12.6 from RyR2, as ''RyR2 (−FKBP)''.

Cryoelectron microscopy and image processing

Cryoelectron micrographs were recorded at 38,800× magnification on a Philips (Eindhoven, The Netherlands) EM 420 transmission electron microscope operated at 100 kV and equipped with a low-dose kit and a GATAN (model 626) cryo-transfer holder. The defocus range for micrographs was 2.0–2.5 μm underfocus. Some micrographs were recorded with the grid at 0° tilt and others with the grid tilted by 30°, so as to obtain adequate sampling of orientations of the RyR complexes. Micrographs were selected for image processing as described previously (53) and then digitized on a Eurocore Hi-Scan microdensitometer (Saint-Denis, France) with a 25-μm step size, corresponding to 5.23 Å on the object scale. For RyR2 (+FKBP), 2095 particle images, and for control RyR2 (−FKBP), 1227 good particle images were selected, after manual screening of images. Reduction of ''bad'' particles (53) was done by setting the threshold of cross correlation so as to eliminate 25% of the particles, thereby improving the homogeneity of the data set. SPIDER software (54) was implemented to obtain the 3D reconstruction by the projection-matching technique (53,55). The final resolution of both reconstructions was estimated to be 33 Å by Fourier shell correlation, with the cutoff of 0.5 (56). To obtain the FKBP12.6 density present in RyR2 (+FKBP12.6), a difference map was computed by subtracting the 3D map of RyR2 (−FKBP12.6) from the RyR2 (+FKBP12.6) map, and density mass obtained was displayed at the same threshold as the 3D maps of RyR2 complexes. The corresponding cryo-density for FKBP12.6 was fitted with x-ray structure of FKBP12.6, filtered to the same resolution as 3D of RyR2. Since the FKBP12.6 x-ray structure is a complex with rapamycin, coordinates of rapamycin were removed from the pdb file and only FKBP12.6 coordinates were used for our docking that was done by using ''O'' software (57), and visualized by using ''Ribbons'' (58) and ''IRIS EXPLORER'' (Numerical Algorithms Group, Downer Grove, IL).

RESULTS

Biochemical and functional characterization of purified RyR2 from dog heart sarcoplasmic reticulum

We have described a new method of purification of RyR2 from dog heart SR using an affinity-purified sequence-specific selective antibody to RyR2. The binding of RyR2 to the Ab/protein A/G matrix was similar to RyR3 as described earlier (49). The elution of purified RyR2 from the immune complex with the use of peptide epitope yielded the purified eluate of RyR2 of high purity as viewed by SDS-PAGE, specific ryanodine binding, and cryo-EM. Western blot analysis confirmed that the peptide eluates from the immune precipitate contained highly purified RyR2. The yield of RyR2 as determined by densitometry was ~25–30 μg protein, from ~100 mg of starting dog heart SR. The yield can be improved by using more affinity-purified antibody to purify the RyR2. The amount used is a practical compromise.

The ryanodine binding of the purified RyR2 receptor was 300–355 pmols/mg of protein measured at 60 nM ryanodine. This is about a 110-fold enrichment from the starting dog heart SR, which shows high affinity binding of ~2.5 pmoles/mg protein. This value indicates that the RyR2 is highly purified and functional with respect to ryanodine binding. Homogeneously pure and functional RyR2, calculated from the known sequence, has a predicted B_{max} ~450 pmols/mg protein. Cryo-EM further confirmed that the RyR2 purified

by the immunoaffinity method was of high purity and was structurally intact (see Results below).

The buffer conditions (see Materials and Methods) used in this study is expected to favor the open state of the receptor (51,59). We chose these conditions, as opposed to ''closed'' conditions (closed conditions include submicromolar [Ca^{2+}], no nucleotide (51), such as were used in our previous cryo-EM analysis of RyR2 (53)), because the structural integrity of the receptors, as judged from the appearance of the images, appeared to be better when the receptor was isolated in the presence of activating ligands (such as nucleotide or epitope, see Meissner (51) for details). We previously noted a similar improved structural stability under open as compared to closed buffer conditions for ryanodine receptor isoform, RyR3 (59).

The best results were obtained when we incubated purified RyR2 with an excess of FKBP12.6 (ratio of RyR2/FKBP12.6 to be ~1:30) in the presence and in the absence of the FKBP12.6-dissociating drug FK506, respectively (see Materials and Methods and also see Kaftan et al. (19)), receptors prepared by these two conditions will henceforth be referred to as RyR2 (−FKBP) and RyR2 (+FKBP)). Confirmation that the desired complexes were obtained was achieved by immunoprecipitation using RyR-specific antibody followed by Western blotting to detect coprecipitated FKBP12.6 (see Supplemental Fig. S1).

Structure of the RyR2-FKBP12.6 complex

Structures of RyR2 (+FKBP12.6) and RyR2 (−FKBP12.6) complexes were obtained using cryo-EM and image processing as described in Materials and Methods. The overall appearances of the resulting 3D reconstructions for RyR2 (+FKBP) and RyR2 (−FKBP) are illustrated as surface representations (Fig. 1, *A* and *B*), which are displayed at a threshold to match the molecular mass of receptor by taking into account the protein density of 1.22 g cm^{-3} (60). Similarly, the difference map was displayed at the same threshold as the receptor (Fig. 1 *B*), and each of the densities attributed to FKBP12.6 corresponds approximately to the molecular mass of FKBP12.6.

As described previously for RyR2, as well as for RyR1 and RyR3, the receptor comprises two main structural components: a transmembrane assembly representing <1/5 of the total mass, and a multidomain cytoplasmic assembly (Fig. 1, *A* and *B*, domains labeled 1–10) representing the main mass (61,62). Not surprisingly, the reconstructions shown in Fig. 1 are similar to previous reconstructions of RyRs, but they differ subtly from one another in several regions that we believe are of significance. As described below, not all of the differences appear to be attributable to extra mass density of the bound FKBP12.6 expected to be present in the RyR2 (+FKBP) but not in RyR2 (−FKBP); we infer that these arise from conformational differences present between the two complexes.

One major difference between the RyR2 (+FKBP) and RyR2 (−FKBP) structures occurs in domain 6, which in RyR2 (+FKBP) appears to be more extended (''stretched'') in the vertical direction (when the receptor is viewed from the side) (Fig. 1, *A* and *B*, *rightmost panels*). Also apparent are alterations in the transmembrane assembly; these give the appearance of a ~4° rotation between RyR2 (+FKBP) and RyR2 (−FKBP) when the structures are viewed from the SR-interacting face (Fig. 1, *center panels*). Both of these differences are similar to structural differences between putatively open and closed forms of RyR1 (and also of RyR3) that have been described previously (59,63). Thus, RyR2 (+FKBP) appears similar in configuration to the open forms of RyR1 and RyR3, whereas RyR2 (−FKBP) resembles the closed form of the receptors. In an earlier study we

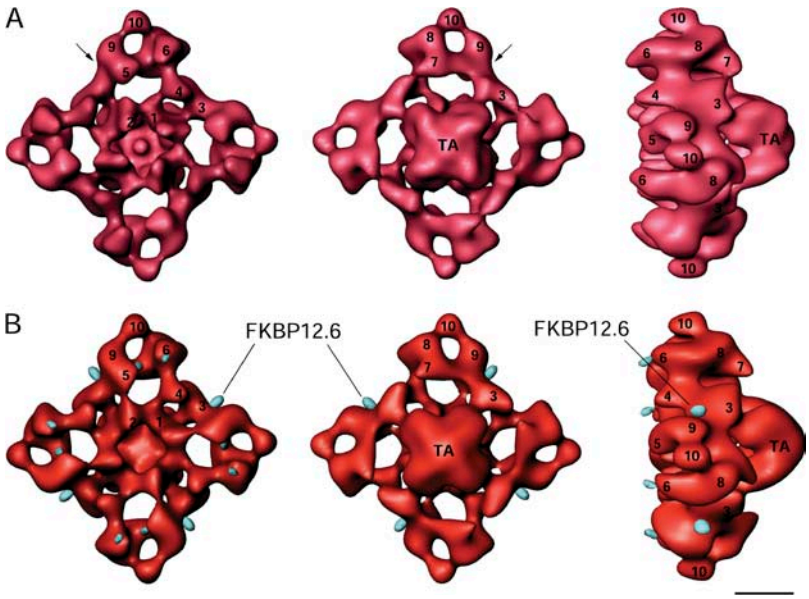

FIGURE 1 Surface representations of 3D cryo-EM reconstructions of RyR2 with and without bound FKBP12.6. (*A*) The 3D map of RyR2 (+FKBP), obtained by assembly in vitro of purified RyR2 incubated with FKBP12.6 alone, and (*B*) the 3D map of RyR2 (−FKBP), obtained by incubating RyR2 with FKBP12.6 and excess FK506, with the superimposed map of difference density (shown in *blue*), as obtained by subtracting the 3D map of RyR2 (−FKBP) from that of RyR2 (+FKBP). In panel *A*, arrows point to the extra density in RyR2 (+FKBP12.6) that accounts for the FKBP12.6 mass that is enhanced in the difference map shown in panel *B*. The 3D volumes for the two conditions are each shown in three views: left, cytoplasmic view; middle, SR junctional face; and right, side view. Abbreviation: TA, transmembrane assembly. Numerals refer to established nomenclature of domains. Scale bar ~100 Å.

determined a 3D reconstruction for RyR2 under conditions that favored the closed state of the channel (53), and that reconstruction was similar to the RyR2 (−FKBP) reconstruction obtained in this study, with respect to the configurations of domain 6 and the transmembrane assembly as has been shown for the closed state of RyR3 (59) (*thumbnail* at *lower left* of Fig. 2). Thus, it appears that RyR2 (−FKBP) assumed a conformation resembling that of the closed conformation. This is an unanticipated result, since both the RyR2 (+FKBP) and RyR2 (−FKBP) reconstructions were computed from specimens under buffer conditions that should have favored the open form of the receptor (see Discussion for further elaboration of this interpretation).

The differences between the two reconstructions that were discussed above, which we attribute to conformational differences between RyR2 (+FKBP) and RyR2 (−FKBP), complicate the localization of the bound FKBP12.6, which was the major objective of this study. Nevertheless, a difference map (Fig. 1 *B*, *blue* density), obtained by subtraction of the RyR2 (−FKBP) volume from that of RyR2 (+FKBP), shows that there are two main sites of positive difference between the reconstructions (representing mass present in RyR2 (+FKBP) that is absent from RyR2 (−FKBP)), each repeated four times as expected for the tetrameric receptor. The difference due to the extension of domain 6 is already discussed, as well as a discrete difference maximum that maps to the interface between domains 3 and 9. The latter difference certainly corresponds to the bound FKBP12.6 (for justification see Discussion). The apparent overall volume of the difference attributed to FKBP12.6 is approximately that expected for a 12.6-kDa protein.

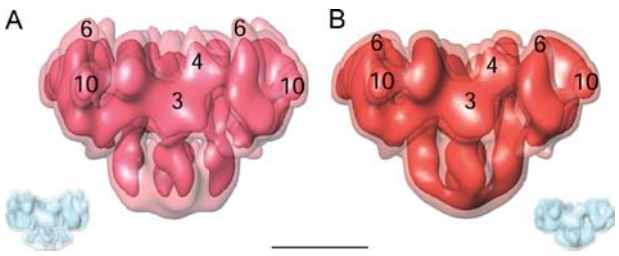

FIGURE 2 3D maps of RyR2 (+FKBP) and RyR2 (−FKBP) shown at two different contour levels with a previously determined structure of RyR3 (59). (*A*) Two superimposed volumes of RyR2 (+FKBP12.6) are shown, one in semitransparent pink and the other as solid pink. For comparison, the ''open'' RyR3 structure is shown as a thumbnail to the lower left. (*B*) Similarly, as in panel *A*, two volumes of RyR2 (−FKBP12.6) are superimposed, one shown in solid red and the other as semitransparent red. The comparative structure of RyR3 in the ''closed'' state is shown as a thumbnail to the lower right. For both panels *A* and *B*, the semitransparent structures are displayed at the same threshold as in Fig. 1, whereas the solid densities of both complexes are shown at a higher threshold such that their total volume is ~1/4 of the semitransparent map. Note the similar conformations of the domains ''6'' in (RyR2 -FKBP12.6) complexes and changes in transmembrane assembly that correlate to RyR3 volumes, respectively. Scale bar ~100 Å.

DISCUSSION

RyR2 purification and Cryo-EM

It is known that Cryo-EM density maps are crucial in elucidating the details of interactions and structural/functional conformational changes associated with ligand binding even for complexes such as ribosomes, for which atomic models have been solved (64,65). In this study, a new method of purification of canine heart RyR2 that makes use of an affinity-purified polyclonal antibody directed against an 11 amino acid peptide epitope of RyR2 (amino acid residues 4418–4429) has been described. The heart SR is solubilized with CHAPS, and the RyR2 is immunoprecipitated using the affinity-purified polyclonal antibody. Purified RyR2 is then gently eluted using peptide epitope, as previously described for the purification of RyR3 (49). The advantages of the new procedure for RyR2 are that it is less laborious than methods employing gradient centrifugation and it yields receptors that are functional and structurally intact for cryo-EM and image processing.

Location of FKBP12.6 binding sites on RyR2

Evidence from previous biochemical studies have shown that maximally ~4 moles of FKBP12.6 bind per mole of RyR2 tetramer (5,6). Here we have determined the location of FKBP12.6 binding on the structure of RyR2 by cryo-EM and single-particle 3D reconstruction techniques. This was accomplished by obtaining and comparing two independent 3D reconstructions, one under conditions where FKBP12.6 should bind to the receptor, and the other in the presence of the drug FK506, which should result in the dissociation of FKBP12.6 from the receptor. The complexes were prepared in buffers containing Ca^{2+} and nucleotide, which are expected to favor the open state of the receptor. Unexpectedly, several differences were found between the two reconstructions that complicated a straightforward interpretation of the FKBP12.6-binding location. Nevertheless, we attribute one of the two principal differences, the one occurring near the junction of domains 9 and 3, to bound FKBP12.6. Since RyR2 is a homotetramer, this difference is repeated four times in the reconstruction (Fig. 1 *B*).

We are confident that our interpretation of FKBP12.6's location is correct for the following reasons. First, this site is located in the same vicinity as the site where the homologous binding protein, FKBP12, binds to RyR1 (44). Since there is high homology between the two FK506-binding protein isoforms (66) as well as between the two RyR isoforms (3), it is likely that the mode of binding will be similar in the two cases. Second, the location of amino acid Thr-1874 is on domain 9 of RyR2, and evidence has been reported that the FKBP12.6 binding site involves amino acid residues in this vicinity, specifically residues 1815–1855 (47). Those findings are consistent with our assignment of the FKBP12.6 binding site because the Thr-1874 site is within ~30 Å of the

FKBP12.6 location reported here. Third, the density differences between RyR2 (+FKBP) and RyR2 (−FKBP) that we do not believe are contributed by bound FKBP12.6 can be explained as arising from conformational differences between the RyR2 structures in the two reconstructions (discussed below).

The FKBP12.6 binding site on RyR2 is similar to that found previously for FKBP12 binding to RyR1 (45,46), but the two sites appear to differ slightly in location by 10–20 Å (for a comparative figure refer to Supplemental Fig. S2). Although this apparent shift could be due to actual differences in the modes of binding of FKBP12.6 and FKBP12, as has been hypothesized recently on the basis of apparent differences in the binding specificities of the two proteins (46,47), it is premature to assign any significance to this difference for the following reasons. Our previous study of the RyR1-FKBP12 complex was performed under conditions that favored the ''closed'' state of RyR1, whereas this study of RyR2 (+FKBP) was done under conditions promoting the ''open'' state. Therefore, the apparent difference in the binding-site location of FKBP12 and FKBP12.6 could be due to conformational differences between open and closed states of the receptors; indeed, movements of domain 9 (a domain which contributes to, or is adjacent to, the FKBP binding sites) in transitions between closed to open states have been documented previously for RyR1 and RyR3 (59,67). Alternatively or additionally, inherent structural differences between the RyR1 and RyR2 isoforms could account for the difference in the binding-site locations; in this regard it should be noted that one of the three regions in which the receptor isoforms' sequences are highly divergent (specifically, divergent region 3, involving RyR1 amino acid residues 1872–1903) is probably near to the FKBP binding region (47).

Currently, the resolutions of our reconstructions limit our ability to uniquely fit the atomic structure of an FKBP12.6-rapamycin complex (68) into our map. We have therefore manually placed a ribbon representation of the structure of FKBP12.6 into the cryo-EM density map in an orientation that fits the difference density reasonably well and which is consistent with available biochemical information (Fig. 3). The docking places amino acid residues Gln-31 and Asn-32 of FKBP12.6, which have been shown by site-directed mutagenesis to be important in FKBP12.6's interaction with RyR2 (8), near the surface of RyR2 (Fig. 3). Phe-59, which has also been implicated in the FKBP12.6-RyR2 interaction, lies in the crystal structure at the base of a hydrophobic cavity that binds the drugs FK506 and rapamycin. Although the drug-binding pocket faces RyR2 in our fitting, Phe-59 appears to be ~10 Å from the apparent surface of RyR2; thus, its role in the interaction of FKBP12.6 with RyR2 may be indirect. Two other residues that are associated with the drug-binding region and that have been proposed to contribute to binding specificity are Ala-63 and Ile-90 (68), and, similarly to Phe-59, they appear displaced from RyR2's surface. If we assume that our docking of FKBP12.6 is approximately accurate, some of the amino acid residues immediately downstream of Asn-32 and extending to approximately Arg-42, which make up a β-sheet and a surface-exposed loop (Fig. 3), could further contribute to the interaction with RyR2. Future studies by site-directed mutagenesis are needed to test this prediction. Note that some of these residues are separated from Gln-31 and Asn-32 by up to 20 Å. Thus, the binding ''footprint'' of FKBP12.6 on RyR2 is sufficiently large to allow several separated regions of RyR2's amino acid sequence to be involved in binding FKBP12.6 (e.g., Ile-Pro residues 2427 and 2428 as well as the region contained within residues 1815–1855), as proposed by Zhang and colleagues (47).

Structure of the RyR2 under open state conditions

Both the RyR (+FKBP) and RyR (−FKBP) 3D reconstructions were determined using buffer conditions that should favor the open state of the receptor. The reconstruction of RyR (+FKBP) indeed displays some structural features that differ from our previous reconstruction of RyR2 prepared under closed conditions (53) and that are characteristic of the open forms that have been reconstructed previously for the

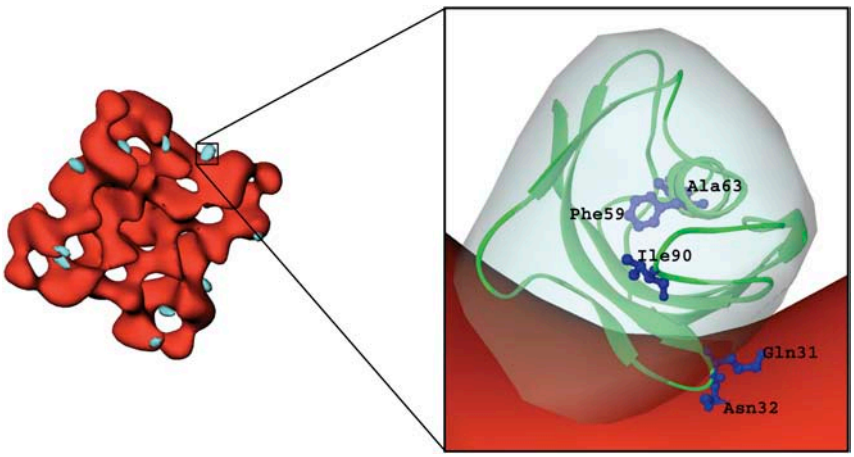

FIGURE 3 Manual docking of FKBP12.6 atomic structure (68) into the 3D density difference map. To the left, a reconstruction of the RyR2 (−FKBP) complex is shown with the difference density map (*blue*), attributed to FKBP12.6, superimposed (*blue;* also see Fig. 1). To the right is an enlargement of one of the four FKBP12.6 difference masses with a ribbon representation of the FKBP12.6 atomic structure (68) docked inside it. To obtain an optimal fitting, the difference map density is displayed at a slightly lower threshold as that shown in Fig. 1 *B*, keeping the maximum limit of the difference density close to the known molecular mass of FKBP12.6. Side chains of residues of interest (Ala-63, Phe-59, Ile-90, Gln-31, and Asn-32) are shown in dark blue (see text).

other receptor isoforms, RyR1 (67) and RyR3 (59). Surprisingly, however, the reconstruction of RyR2 (−FKBP) does not show such characteristics; instead, its 3D structure more closely resembles structures of RyR isoforms, including RyR2, in the closed state (53,59,67). Two of the main features that distinguish open from closed receptors (which can be seen by comparing Fig. 2 *A* (RyR (+FKBP), putatively open) with Fig. 2 *B* (RyR2 (−FKBP), putatively closed)) are an elongation of cytoplasmic domain 6 along a direction approximately parallel to the receptor's fourfold symmetry axis (Fig. 2, *A* and *B*, *rightmost panels*) and a splaying apart of elongate high-density regions within the transmembrane region. In Fig. 2, these changes are illustrated for RyR2-FKBP12.6 complexes and for reference, open and closed forms of RyR3 from previous work (59) are also shown (as *thumbnails*). It should be appreciated that the conformational changes associated with domain 6 are distant, well over 100 Å, from the cytoplasmically exposed entrance to the ion channel, which is presumably located near the center of the receptor, near the junction of the cytoplasmic and transmembrane regions.

Significance of RyR2 (−FKBP) structure

An unexpected result was that the 3D reconstruction of RyR2 (−FKBP) resembles more closely a reconstruction of the closed state of the receptor, even though open-promoting conditions were used for the experiment (69). On the other hand, the reconstruction of RyR (+FKBP) does exhibit features characteristic of the open state (see above), as expected. The main functional effect of FKBP12.6/FKBP12 binding to RyR2/RyR1 is frequently described as a stabilization of the closed state of the receptor, because when FKBP12.6/FKBP12 is removed from the receptors they periodically open for brief intervals in the absence of channel activators (70). If destabilization of the closed state is indeed the main functional effect of removing FKBP12.6, then one might have expected the 3D map of RyR2 (−FKBP) to be in the open state.

How, then, do we account for our finding that the RyR2 (−FKBP) structure resembles the closed state? We hypothesize that this structure depicts a state of the receptor that is neither fully open nor closed. An effect of removal of FKBP12/FKBP12.6 from RyR1/RyR2 is that frequently when channel openings do occur after addition of channel activators, the conductance of the channels is reduced to a constant fraction of the fully open state (15,19). However, these subconductance states have not been observed by all workers (21), and it has been suggested that such states might arise due to a secondary direct interaction of FK506 (or rapamycin) with RyR1/RyR2, particularly in cases where RyR2 is exposed for extended durations (>20 min) or to elevated levels of the drug (50 μM); both of these conditions applied in our study (21). Our working hypothesis is that the 3D structure of FK506-treated RyR2 in the presence of channel activators depicts the receptor in a configuration that corresponds to a subconductance state, rather than to the open state; if this is so, then our results indicate that the structure of this subconductance state is more similar to that of the closed than to that of the open state.

In summary, we have found that 1) FKBP12.6 binds to RyR2 at a site close to that found on RyR1 for FKBP12, and 2) RyR2 depleted of FKBP12.6 by drug treatment has a different conformation from that with FKBP12.6 present. Future studies of additional RyR-FKBP complexes and at higher resolution will be necessary to determine 1) whether there are any significant differences in the binding modes of FKBP12.6 and FKB12 to RyR isoforms, and 2) the precise conformational changes of RyR2 induced by FKBP12.6 depletion.

SUPPLEMENTARY MATERIAL

An online supplement to this article can be found by visiting BJ Online at http://www.biophysj.org.

We thank the Wadsworth Center's Electron Microscopy core facility and gratefully acknowledge support by grants AR40615 and RR01219 from the National Institutes of Health. L.H.J. was supported, in part, by National Institutes of Health National Research Service Award Institutional Training Grant 5 T32 HL07411-19.

REFERENCES

1. Bers, D. M. 2004. Macromolecular complexes regulating cardiac ryanodine receptor function. *J. Mol. Cell. Cardiol.* 37:417–429.
2. Fill, M., and J. A. Copello. 2002. Ryanodine receptor calcium release channels. *Physiol. Rev.* 82:893–922.
3. Sorrentino, V., and P. Volpe. 1993. Ryanodine receptors—how many, where and why? *Trends Pharmacol. Sci.* 14:98–103.
4. Jayaraman, T., A. M. Brillantes, A. P. Timerman, S. Fleischer, H. Erdjument-Bromage, P. Tempst, and A. R. Marks. 1992. FK506 binding protein associated with the calcium release channel (ryanodine receptor). *J. Biol. Chem.* 267:9474–9477.
5. Jeyakumar, L. H., L. Ballester, D. S. Cheng, J. O. McIntyre, P. Chang, H. E. Olivey, L. Rollins-Smith, J. V. Barnett, K. Murray, H. B. Xin, and S. Fleischer. 2001. FKBP binding characteristics of cardiac microsomes from diverse vertebrates. *Biochem. Biophys. Res. Commun.* 281:979–986.
6. Timerman, A. P., H. Onoue, H.-B. Xin, S. Barg, J. Copello, G. Wiederrecht, and S. Fleischer. 1996. Selective binding of FKBP12.6 by cardiac ryanodine receptor. *J. Biol. Chem.* 271:20385–20391.
7. Timerman, A. P., E. Ogunbumni, E. Freund, G. Wiederrecht, A. R. Marks, and S. Fleischer. 1993. The calcium release channel of sarcoplasmic reticulum is modulated by FK-506-binding protein. Dissociation and reconstitution of FKBP-12 to the calcium release channel of skeletal muscle sarcoplasmic reticulum. *J. Biol. Chem.* 268: 22992–22999.
8. Xin, H.-B., K. Rogers, Y. Qi, T. Kanematsu, and S. Fleischer. 1999. Three amino acid residues determine selective binding of FK506-binding protein 12.6 to the cardiac ryanodine receptor. *J. Biol. Chem.* 274:15315–15319.
9. Aizawa, Y., K. Ueda, S. Komura, T. Washizuka, M. Chinushi, N. Inagaki, Y. Matsumoto, T. Hayashi, M. Takahashi, N. Nakano, M. Yasunami, A. Kimura, M. Hiraoka, and Y. Aizawa. 2005. A novel

mutation in FKBP12.6 binding region of the human cardiac ryanodine receptor gene (R2401H) in a Japanese patient with catecholaminergic polymorphic ventricular tachycardia. *Int. J. Cardiol.* 99:343–345.

10. Bers, D. M., D. A. Eisner, and H. H. Valdivia. 2003. Sarcoplasmic reticulum Ca^{2+} and heart failure: roles of diastolic leak and Ca^{2+} transport. *Circ. Res.* 93:487–490.
11. Marks, A. R. 2003. A guide for the perplexed: towards an understanding of the molecular basis of heart failure. *Circulation.* 107:1456–1459.
12. Wehrens, X. H., S. E. Lehnart, F. Huang, J. A. Vest, S. R. Reiken, P. J. Mohler, J. Sun, S. Guatimosim, L. S. Song, N. Rosemblit, J. M. D'Armiento, C. Napolitano, M. Memmi, S. G. Priori, W. J. Lederer, and A. R. Marks. 2003. FKBP12.6 deficiency and defective calcium release channel (ryanodine receptor) function linked to exercise-induced sudden cardiac death. *Cell.* 113:829–840.
13. Ahern, G. P., P. R. Junankar, and A. F. Dulhunty. 1994. Single channel activity of the ryanodine receptor calcium release channel is modulated by FK-506. *FEBS Lett.* 352:369–374.
14. Ahern, G. P., P. R. Junankar, and A. F. Dulhunty. 1997. Subconductance states in single-channel activity of skeletal muscle ryanodine receptors after removal of FKBP12. *Biophys. J.* 72:146–162.
15. Brillantes, A. B., K. Ondrias, A. Scott, E. Kobrinsky, E. Ondriašová, M. C. Moschella, T. Jayaraman, M. Landers, B. E. Ehrlich, and A. R. Marks. 1994. Stabilization of calcium release channel (ryanodine receptor) function by FK506-binding protein. *Cell.* 77:513–523.
16. Chen, S. R. W., L. Zhang, and D. H. MacLennan. 1994. Asymmetrical blockade of the Ca^{2+} release channel (ryanodine receptor) by 12-kDa FK506 binding protein. *Proc. Natl. Acad. Sci. USA.* 91:11953–11957.
17. El-Hayek, R., A. J. Lokuta, C. Arévalo, and H. H. Valdivia. 1995. Peptide probe of ryanodine receptor function. *J. Biol. Chem.* 270: 28696–28704.
18. Mayrleitner, M., A. P. Timerman, G. Wiederrecht, and S. Fleischer. 1994. The calcium release channel of sarcoplasmic reticulum is modulated by FK-506 binding protein—effect of FKBP-12 on single channel activity of the skeletal muscle ryanodine receptor. *Cell Calcium.* 15:99–108.
19. Kaftan, E., A. R. Marks, and B. E. Ehrlich. 1996. Effects of rapamycin on ryanodine receptor/Ca^{2+}-release channels from cardiac muscle. *Circ. Res.* 78:990–997.
20. Xiao, R. P., H. H. Valdivia, K. Bogdanov, C. Valdivia, E. G. Lakatta, and H. Cheng. 1997. The immunophilin FK506-binding protein modulates Ca2+ release channel closure in rat heart. *J. Physiol. (Lond.).* 500:343–354.
21. Barg, S., J. A. Copello, and S. Fleischer. 1997. Different interactions of cardiac and skeletal muscle ryanodine receptors with FK-506 binding protein isoforms. *Am. J. Physiol. Cell Physiol.* 272:1726–1733.
22. Marx, S. O., K. Ondrias, and A. R. Marks. 1998. Coupled gating between individual skeletal muscle Ca^{2+} release channels (ryanodine receptors). *Science.* 281:818–821.
23. Marx, S. O., J. Gaburjakova, M. Gaburjakova, C. Henrikson, K. Ondrias, and A. R. Marks. 2001. Coupled gating between cardiac calcium release channels (ryanodine receptors). *Circ. Res.* 88:1151–1158.
24. Dulhunty, A. F., D. R. Laver, E. M. Gallant, M. G. Casarotto, S. M. Pace, and S. Curtis. 1999. Activation and inhibition of skeletal RyR channels by a part of the skeletal DHPR II–III loop: effects of DHPR Ser^{687} and FKBP12. *Biophys. J.* 77:189–203.
25. O'Reilly, F. M., M. Robert, I. Jona, C. Szegedi, M. Albrieux, S. Geib, M. D. Waard, M. Villaz, and M. Ronjat. 2002. FKBP12 modulation of the binding of the skeletal ryanodine receptor onto the II–III loop of the dihydropyridine receptor. *Biophys. J.* 82:145–155.
26. Bandyopadhay, A., D. W. Shin, J. O. Ahn, and D. H. Kim. 2000. Calcineurin regulates ryanodine receptor/Ca^{2+}-release channels in rat heart. *Biochem. J.* 352:61–70.
27. Shin, D. W., Z. Pan, A. Bandlyopadhyay, M. B. Bhat, D. H. Kim, and J. J. Ma. 2002. Ca2+-dependent interaction between FKBP12 and calcineurin regulates activity of the Ca2+ release channel in skeletal muscle. *Biophys. J.* 83:2539–2549.
28. Lamb, G. D., and D. G. Stephenson. 1996. Effects of FK506 and rapamycin on excitation-contraction coupling in skeletal muscle fibres of the rat. *J. Physiol. (Lond.).* 494:569–576.
29. Avila, G., E. H. Lee, C. F. Perez, P. D. Allen, and R. T. Dirksen. 2003. FKBP12 binding to RyR1 modulates excitation-contraction coupling in mouse skeletal myotubes. *J. Biol. Chem.* 278:22600–22608.
30. Xin, H. B., T. Senbonmatsu, D. S. Cheng, Y. X. Wang, J. A. Copello, G. J. Ji, M. L. Collier, K. Y. Deng, L. H. Jeyakumar, M. A. Magnuson, T. Inagami, M. I. Kotlikoff, and S. Fleischer. 2002. Oestrogen protects FKBP12.6 null mice from cardiac hypertrophy. *Nature.* 416:334–337.
31. Marx, S. O., S. Reiken, Y. Hisamatsu, T. Jayaraman, D. Burkhoff, N. Rosemblit, and A. R. Marks. 2000. PKA phosphorylation dissociates FKBP12.6 from the calcium release channel (ryanodine receptor): defective regulation in failing hearts. *Cell.* 101:365–376.
32. Doi, M., M. Yano, S. Kobayashi, M. Kohno, T. Tokuhisa, S. Okuda, M. Suetsugu, Y. Hisamatsu, T. Ohkusa, M. Kohno, and M. Matsuzaki. 2002. Propranolol prevents the development of heart failure by restoring FKBP12.6-mediated stabilization of ryanodine receptor. *Circulation.* 105:1374–1379.
33. Kohno, M., M. Yano, S. Kobayashi, M. Doi, T. Oda, T. Tokuhisa, S. Okuda, T. Ohkusa, M. Kohno, and M. Matsuzaki. 2003. A new cardioprotective agent, JTV519, improves defective channel gating of ryanodine receptor in heart failure. *Am. J. Physiol. Heart Circ. Physiol.* 284:1035–1042.
34. Yano, M., K. Ono, T. Ohkusa, M. Suetsugu, M. Kohno, T. Hisaoka, S. Kobayashi, Y. Hisamatsu, T. Yamamoto, N. Noguchi, S. Takasawa, H. Okamoto, and M. Matsuzaki. 2000. Altered stoichiometry of FKBP12.6 versus ryanodine receptor as a cause of abnormal Ca^{2+} leak through ryanodine receptor in heart failure. *Circulation.* 102:2131–2136.
35. Laitinen, P. J., K. M. Brown, K. Piippo, H. Swan, J. M. Devaney, B. Brahmbhatt, E. A. Donarum, M. Marino, N. Tiso, M. Viitasalo, L. Toivonen, D. A. Stephan, and K. Kontula. 2001. Mutations of the cardiac ryanodine receptor (RyR2) gene in familial polymorphic ventricular tachycardia. *Circulation.* 103:485–490.
36. Priori, S. G., C. Napolitano, N. Tiso, M. Memmi, G. Vignati, R. Bloise, V. Sorrentino, and G. A. Danieli. 2001. Mutations in the cardiac ryanodine receptor gene (*hRyR2*) underlie catecholaminergic polymorphic ventricular tachycardia. *Circulation.* 103:196–200.
37. Tiso, N., D. A. Stephan, A. Nava, A. Bagattin, J. M. Devaney, F. Stanchi, G. Larderet, B. Brahmbhatt, K. Brown, B. Bauce, M. Muriago, C. Basso, G. Thiene, G. A. Danieli, and A. Rampazzo. 2001. Identification of mutations in the cardiac ryanodine receptor gene in families affected with arrhythmogenic right ventricular cardiomyopathy type 2 (ARVD2). *Hum. Mol. Genet.* 10:189–194.
38. Tiso, N., M. Salamon, A. Bagattin, G. A. Danieli, F. Argenton, and M. Bortolussi. 2002. The binding of the RyR2 calcium channel to its gating protein FKBP12.6 is oppositely affected by ARVD2 and VTSIP mutations. *Biochem. Biophys. Res. Commun.* 299:594–598.
39. George, C. H., G. V. Higgs, and F. A. Lai. 2003. Ryanodine receptor mutations associated with stress-induced ventricular tachycardia mediate increased calcium release in stimulated cardiomyocytes. *Circ. Res.* 93:531–540.
40. Bultynck, G., D. Rossi, G. Callewaert, L. Missiaen, V. Sorrentino, J. B. Parys, and H. De Smedt. 2001. The conserved sites for the FK506-binding proteins in ryanodine receptors and inositol 1,4,5-trisphosphate receptors are structurally and functionally different. *J. Biol. Chem.* 276:47715–47724.
41. Gaburjakova, M., J. Gaburjakova, S. Reiken, F. Huang, S. O. Marx, N. Rosemblit, and A. R. Marks. 2001. FKBP12 binding modulates ryanodine receptor channel gating. *J. Biol. Chem.* 276:16931–16935.
42. Sharma, M. R., and T. Wagenknecht. 2004. Electron microscopy and 3D reconstruction of ryanodine receptors and its interactions with E-C coupling proteins. *Basic Appl. Myol.* 14:299–306 [Review].
43. Wagenknecht, T., R. Grassucci, J. Berkowitz, G. J. Wiederrecht, H.-B. Xin, and S. Fleischer. 1996. Cryoelectron microscopy resolves

FK506-binding protein sites on the skeletal muscle ryanodine receptor. *Biophys. J.* 70:1709–1715.

44. Wagenknecht, T., M. Radermacher, R. Grassucci, J. Berkowitz, H.-B. Xin, and S. Fleischer. 1997. Locations of calmodulin and FK506-binding protein on the three-dimensional architecture of the skeletal muscle ryanodine receptor. *J. Biol. Chem.* 272:32463–32471.
45. Zissimopoulos, S., and F. A. Lai. 2005. Interaction of FKBP12.6 with the cardiac ryanodine receptor c-terminal domain. *J. Biol. Chem.* 280: 5475–5485.
46. Masumiya, H., R. Wang, J. Zhang, B. Xiao, and S. R. Wayne Chen. 2003. Localization of the 12.6-kDa FK506-binding protein (FKBP12.6) binding site to the NH_2-terminal domain of the cardiac Ca^{2+} release channel (ryanodine receptor). *J. Biol. Chem.* 278:3786–3792.
47. Zhang, J., Z. Liu, H. Masumiya, R. Wang, D. Jiang, F. Li, T. Wagenknecht, and S. R. Wayne Chen. 2003. Three-dimensional localization of divergent Region 3 of the ryanodine receptor to the clamp-shaped structures adjacent to the FKBP binding sites. *J. Biol. Chem.* 278:14211–14218.
48. Hakamata, Y., J. Nakai, H. Takeshima, and K. Imoto. 1994. Primary structure and distribution of a novel ryanodine receptor/calcium release channel from rabbit brain. *FEBS Lett.* 312:229–235.
49. Jeyakumar, L. H., J. A. Copello, A. M. O'Malley, G.-M. Wu, R. Grassucci, T. Wagenknecht, and S. Fleischer. 1998. Purification and characterization of ryanodine receptor 3 from mammalian tissue. *J. Biol. Chem.* 273:16011–16020.
50. Chamberlain, B. K., D. O. Levitsky, and S. Fleischer. 1983. Isolation and characterization of canine cardiac sarcoplasmic reticulum with improved Ca2+ transport properties. *J. Biol. Chem.* 258:6602–6609.
51. Meissner, G. 2002. Regulation of mammalian ryanodine receptors. *Front. Biosci.* 7:d2072–2080.
52. Lam, E., M. M. Martin, A. P. Timerman, C. Sabers, S. Fleischer, T. Lukas, Abraham, R., O'Kefe, S.J., O'Neil, E.A., and Wiederrecht, G.J. 1995. A novel FK506 binding protein can mediate the immunosuppressive effects of FK506 and is associated with the cardiac ryanodine receptor. *J. Biol. Chem.* 270:26511–26522.
53. Sharma, M. R., P. Penczek, R. Grassucci, H.-B. Xin, S. Fleischer, and T. Wagenknecht. 1998. Cryoelectron microscopy and image analysis of the cardiac ryanodine receptor. *J. Biol. Chem.* 273:18429–18434.
54. Frank, J., M. Radermacher, P. Penczek, J. Zhu, Y. Li, M. Ladjadj, and A. Leith. 1996. SPIDER and WEB: processing and visualization of images in 3D electron microscopy and related fields. *J. Struct. Biol.* 116:190–199.
55. Penczek, P. A., R. A. Grassucci, and J. Frank. 1994. The ribosome at improved resolution—new techniques for merging and orientation refinement in 3D cryo-electron microscopy of biological molecules. *Ultramicroscopy.* 53:251–270.
56. Malhotra, A., P. Penczek, R. K. Agrawal, I. S. Gabashvilli, R. A. Grassucci, R. Jünemann, N. Burkhardt, K. H. Nierhaus, and J. Frank. 1998. *Escherichia coli* 70 S ribosome at 15 Å resolution by cryo-electron microscopy: localization of fMet-$tRNA_f^{Met}$ and fitting of L1 protein. *J. Mol. Biol.* 280:103–116.
57. Jones, T. A., J. Y. Zou, S. W. Cowan, and M. Kjeldgaard. 1991. Improved methods for building protein models in electron density maps and location of errors in these models. *Acta Crystallogr. A.* 47: 110–119.
58. Carson, M. 1991. Ribbons 2.0 J. *Appl. Crystallogr.* 24:103–106.
59. Sharma, M. R., L. H. Jeyakumar, S. Fleischer, and T. Wagenknecht. 2000. Three-dimensional structure of ryanodine receptor isoform three in two conformational states as visualized by cryo-electron microscopy. *J. Biol. Chem.* 275:9485–9491.
60. Quillin, M. L., and B. W. Mathews. 2000. Accurate calculation of the density of proteins. *Acta Crystallogr. D.* 56:791–794.
61. Radermacher, M., V. Rao, R. Grassucci, J. Frank, A. P. Timerman, S. Fleischer, and T. Wagenknecht. 1994. Cryo-electron microscopy and three-dimensional reconstruction of the calcium release channel ryanodine receptor from skeletal muscle. *J. Cell Biol.* 127:411–423.
62. Serysheva, I. I., E. V. Orlova, W. Chiu, M. B. Sherman, S. L. Hamilton, and M. van Heel. 1995. Electron cryomicroscopy and angular reconstitution used to visualize the skeletal muscle calcium release channel. *Nat. Struct. Biol.* 2:18–24.
63. Orlova, E. V., I. I. Serysheva, M. van Heel, S. L. Hamilton, and W. Chiu. 1996. Two structural configurations of the skeletal muscle calcium release channel. *Nat. Struct. Biol.* 3:547–552.
64. Agrawal, R. K., M. R. Sharma, M. C. Kiel, G. Hirokawa, T. M. Booth, C. M. Spahn, R. A. Grassucci, A. Kaji, and J. Frank. 2004. Visualization of ribosome-recycling factor on the Escherichia coli 70S ribosome: functional implications. *Proc. Natl. Acad. Sci. USA.* 101: 8900–8905.
65. Gao, H., and J. Frank. 2005. Molding atomic structures into Intermediate- Resolution Cryo-EM density maps of ribosomal complexes using real-space refinement. *Structure (Camb.).* 13:401–406.
66. Sewell, T. J., E. Lam, M. M. Martin, J. Leszyk, J. Weidner, J. Calaycay, P. Griffin, H. Williams, S. Hung, and J. Cryan. 1994. Inhibition of calcineurin by a novel FK-506-binding protein. *J. Biol. Chem.* 269:21094–21102.
67. Serysheva, I. I., M. Schatz, M. van Heel, W. Chiu, and S. L. Hamilton. 1999. Structure of the skeletal muscle calcium release channel activated with Ca^{2+} and AMP-PCP. *Biophys. J.* 77:1936–1944.
68. Devianayagam, C. C. S., M. Carson, A. Thotakura, S. V. L. Narayana, and R. S. Chodavarapu. 2000. Structure of FKBP12.6 in complex with rapamycin. *Acta Crystallogr. D Biol. Crystallogr.* 56:266–271.
69. Anderson, K., F. A. Lai, Q. Y. Liu, E. Rousseau, H. P. Erickson, and G. Meissner. 1989. Structural and functional characterization of the purified cardiac ryanodine receptor-Ca2+ release channel complex. *J. Biol. Chem.* 264:1329–1335.
70. Marks, A. R. 2002. Ryanodine receptors, FKBP12, and heart failure. *Front. Biosci.* 7:d970–977 [Review].